

# Relationship between Solar Wind Parameters and Geomagnetic Activity Indices

Azrin Nur Farhana binti Abdullah Din @ Azman

Faculty of Electrical Engineering, Universiti Teknologi MARA (UiTM), 40450 Shah Alam, Selangor, Malaysia.

E-mail: [ajien\\_anf@yahoo.com](mailto:ajien_anf@yahoo.com)

**Abstract**— This study examined the relationship of solar wind parameters due to geomagnetic activity indices during disturbed period (Coronal Holes events & Coronal Mass Ejection events) and quiet period. In this analysis, for solar wind parameters, we are focusing on Interplanetary Magnetic Field Magnitude (B), Interplanetary Magnetic Field Temperature (T), Proton Density (N), Solar Wind Speed (V<sub>sw</sub>) and Solar Wind Input Energy (ε) while for the geomagnetic indices, polar cap index (PC), auroral electrojet index (AE), disturbance storm time index (Dst) and planetary K-index (Kp) were investigated. The solar wind parameters and geomagnetic indices data are retrieved from OMNIWeb Data Explorer maintained by Goddard Space Flight Center, NASA. The variability of horizontal component of the geomagnetic field at three different latitudes stations extracted from Magnetic Data Acquisition System/Circum-pacific Magnetometer Network (MAGDAS/CPMN) were investigated in order to study the correlation of geomagnetic pulsations with solar wind parameters. Data are supplied by International Center for Space Weather Science and Education, ICSWSE, Kyushu University, Japan. Due to availability of data, the event within 2009 and 2010 period were chosen. From the analysis, both Coronal Holes and Coronal Mass Ejection events show significant relationship with geomagnetic indices and pulsations. However, both solar wind events influence the geomagnetic pulsations, Pc5 according to the geomagnetic stations. Details of the analysis will be discussed throughout this paper.

**Keywords**— Coronal holes, Coronal mass ejection, Geomagnetic indices, Solar wind parameters

## I. INTRODUCTION

### A. Space Weather

Space weather refers to the conditions in interplanetary space, produced by the Sun, that can disrupt modern technologies and affect human life or health [1]. Space weather is driven by solar activity which comprises a wide variety of phenomena such as solar flares, geomagnetic storms and solar energetic particles. Solar flares occurred when there is a sudden increase in electromagnetic radiation. It is an explosion on the Sun's surface caused by the release of magnetic energy in the solar atmosphere. Geomagnetic storms are caused by bulk flows of magnetized plasma from sudden eruptions known as Coronal Mass Ejections (CME) and from solar wind interactions while solar energetic particles are generated by CMEs and flares that accelerate particles to relativistic speeds. Solar energetic particles arrive at Earth between 20 minutes and 24 hours. Storm driven by CME are more common during the increasing and maximum phases of the solar activity while coronal hole are commonly during declining and minimum phases of solar activity.

### B. Coronal Holes (CH) Event

Coronal holes are regions of low density plasma where the sun's corona (outer hot layers of the solar atmosphere) is dark. These darker regions are cooler and were the least active regions of the sun. During low solar activity, coronal holes are mainly found at the sun's North and South polar caps. Unlike the solar minimum period, coronal holes are located anywhere at all solar latitude during the active period of solar cycle [2]. Coronal holes are associated with open magnetic field lines and the acceleration of high speed solar wind. The high speed solar wind is known to originate in coronal holes. The open structure of their magnetic field allows a constant flow of ionized atoms and electrons to stream out of the holes and form the highest speed components of the solar wind. The sources of streams for Coronal holes and Coronal mass ejection can be identified from the differences in the time profiles of plasma speed (V<sub>sw</sub>), IMF temperature (T), proton density (N) and associated magnetic field (B). During CH, enhancement in solar wind speed, V<sub>sw</sub> proceeds relatively slowly to reach its peak and remains enhanced for a longer period before it comes down slowly [3]. The proton density rises to unusually high values near (often preceding) the leading edges of streams due to CH. During CH, proton temperature varies in a pattern similar to the flow speed. Magnetic field and proton density peak before the speed maximum during CH [3].

### C. Coronal Mass Ejection (CME) Event

The most extreme events occurring in our solar system are coronal mass ejections. Coronal mass ejection is a gigantic eruption of plasma and magnetic field being released from the Sun into the corona and interplanetary space. Coronal mass ejections occur when the confined solar atmosphere suddenly and violently bubbles of electrified gas and magnetic fields. CME may initiate spectacular geomagnetic storms if they hit Earth's magnetosphere. They arrive at Earth in 1 to 4 days. They are organized magnetic structures that transfer their energy to Earth's magnetic field [1]. The first CME was detected on December 14, 1971 by the white-light coronagraph on board NASA's seventh Orbiting Solar Observatory (Tousey 1973). CME was found to undergo early acceleration, non-radial motion, angular width expansion, and aerodynamic drag in the solar wind as it propagated towards Earth [4]. Generally it is assumed that fast CMEs ( $V \geq 900$  km s<sup>-1</sup>) are decelerated and slow CMEs ( $V \leq 400$  km s<sup>-1</sup>) are accelerated by the drag force (Yashiro et al. 2004). The sources of streams for Coronal holes and Coronal mass ejection can be identified from the differences in the time profiles of plasma speed (V<sub>sw</sub>), IMF temperature (T), proton

density (N) and associated magnetic field (B). During CME, velocity,  $V_{sw}$  increases at a faster rate to reach its peak and remains enhanced for a shorter period and come down relatively faster. Proton density enhancement is almost simultaneous to velocity enhancement due to CME streams. For the IMF temperature during CME, it becomes low after the initial rise during shock, if present. Peaks in magnetic field (B), proton density (N) and solar wind speed ( $V_{sw}$ ) are near simultaneous during CME [3].

#### D. Geomagnetic Activity Indices

Dependence of geomagnetic activity on various solar wind parameters is characterized using an index measuring the degree of disturbance. A great variety of geomagnetic indices have been proposed and employed over the years. Some of them are specialized indices designed to characterize specific aspects of the total disturbance. For the geomagnetic activity indices, there are four indices that are considered in this studies which are the polar cap index (PC), planetary K-index ( $K_p$ ), disturbance storm time index (Dst), and auroral electrojet index (AE).

The polar cap index is an index for monitoring geomagnetic activity over the polar caps which are due to the changes in the interplanetary magnetic field (IMF) and solar wind. PC index has been introduced by *Troshichev et al.* [1979, 1988] [5].

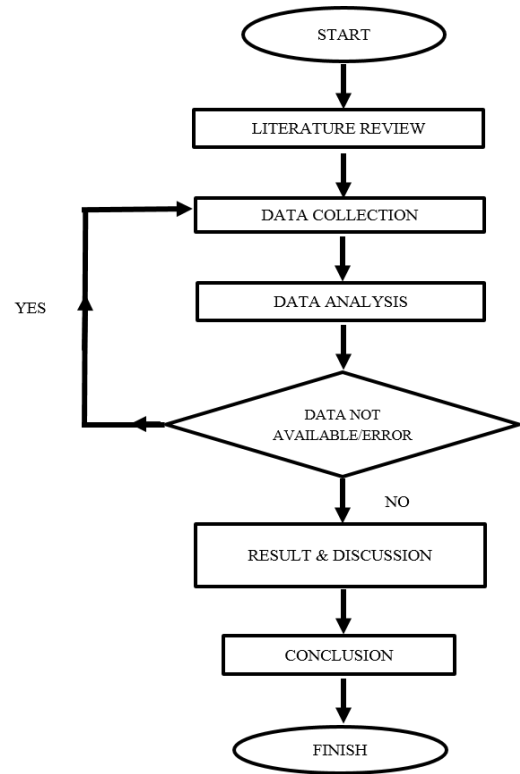
Defined and developed by Davis and Sugiura [1966], the Auroral Electrojet (AE) index was introduced as a measure of global electrojet activity in the auroral zone. The AE index is designed to provide a global, quantitative measure of auroral zone magnetic activity produced by enhanced ionospheric currents flowing below and within the auroral oval [6].

The planetary three-hour-range  $K_p$  index was introduced by J. Bartels in 1949. It is designed to measure solar particle radiation by its magnetic effects. The  $K_p$  index is a global geomagnetic storm index with a scale of 0 to 9 [7].  $K_p$  index is derived from the maximum fluctuations of horizontal components observed on a magnetometer during a three-hour interval. The most important thing to know about aurora watching is the  $k_p$  index.

The Dst index is a global indicator of the state of the Earth's geomagnetic activity used in scientific studies and in defining space weather effects [8]. The Dst index is an index of magnetic activity derived from a network of near-equatorial geomagnetic observatories that measures the intensity of the globally symmetrical equatorial electrojet.

## II. METHODOLOGY

### A. Flowchart



### B. Data and instrumentations

#### i. Solar Wind Parameter And Geomagnetic Indices

The solar wind parameters are supplied by the satellites at the geostationary orbit in the near Earth space whereas the magnetic field variation are recorded by a network of observatories well located all over the world. In this study, all the data for the solar wind parameters and the geomagnetic activity indices are obtained from The Space Physics Data Facility (SPDF) based at NASA's Goddard Space Flight Center in Greenbelt, MD U.S.A. in real time data. The Space Physics Data Facility (SPDF) was constructed for monitoring of the electromagnetic and plasma environment in the geo-space in real-time.

The input data for this database system are supplied from several satellites system such as Interplanetary Monitoring Platform-8 (IMP 8), Interplanetary Physics Laboratory (Wind), Advanced Composition Explorer (ACE), and Geomagnetic Tail Laboratory (Geotail). The OMNI data were retrieved from the GSFC/SPDF OMNIWeb interface at <http://omniweb.gsfc.nasa.gov>. Data obtained from the OMNI database are the hourly values and the gaps in the data were filled by interpolation. The data is plotted using MATLAB programming language.

For each event, the energy transfer to the magnetosphere is estimated by using the original Akasofu parameter.

Akasofu's epsilon parameter is defined as equation (1) [9]:

$$\varepsilon = \frac{4\pi}{\mu_0} VB^2 \sin^4\left(\frac{\theta}{2}\right) l_0^2 \text{ [ergs/s]} \quad (1)$$

Where:-

$V$  = the solar wind speed (km/s)

$B$  = the magnitude of the IMF (nT)

$\theta$  = the polar angle of the IMF vector in the y-z plane in solar-magnetospheric coordinate

$$= \tan^{-1}(|B_y|)/B_z \text{ for } B_z > 0$$

$$= \pi - \tan^{-1}(|B_y|)/B_z \text{ for } B_z < 0$$

$l_0 = 7$  Earth radii.

## ii. Geomagnetic Pulsations

The analysis of geomagnetic pulsations were extracted based on H-direction geomagnetic field data from three (3) MAGDAS stations of different latitudes. The MAGDAS stations that are involved in this research are Davao-DAV (Philippine), Onagawa-ONW (Japan) and Magadan-MGD (Russia) for low, mid and high latitude station respectively. The details of the stations can be referred at Table 1.

Magnetic Data Acquisition System/Circum-pan Pacific Magnetometer Network (MAGDAS/CPMN) is a system deployed by International Center for Space Weather

Science and Education, ICSWSE, Kyushu University, Japan. It consists of 72 realtime magnetometers which covers 3 main unique chains of magnetic observatories; the most magnetometers were densely installed at  $210^\circ$  magnetic meridian, on African longitude-sector and the other one is on the sector along the magnetic equator, as shown in Figure 1.

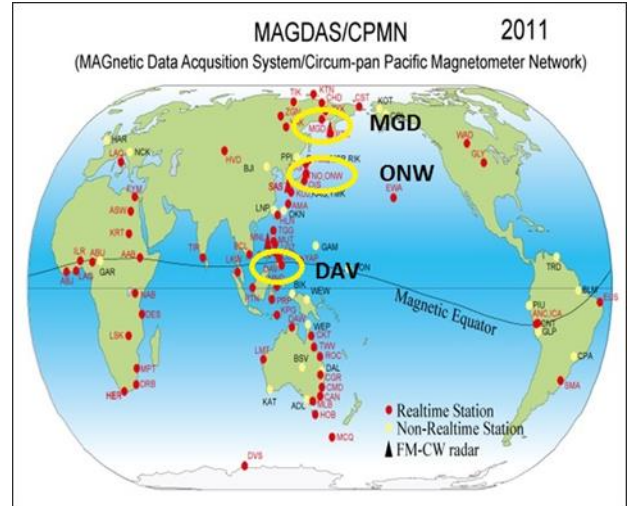


Figure 1: MAGDAS stations map [10]. The marked MAGDAS stations are the geomagnetic observatories involved in this study, form north: MGD (Russia), ONW (Japan) & DAV (Philippine).

TABLE 1: List of MAGDAS observatories stations.

| Station name | Code | Geographic    |                | Geomagnetic   |                |
|--------------|------|---------------|----------------|---------------|----------------|
|              |      | GG lat.       | GG long.       | GM lat.       | GM long.       |
| Magadan      | MGD  | $59.97^\circ$ | $158.25^\circ$ | $53.62^\circ$ | $219.10^\circ$ |
| Onagawa      | ONW  | $38.44^\circ$ | $141.48^\circ$ | $31.27^\circ$ | $212.72^\circ$ |
| Davao        | DAV  | $7.00^\circ$  | $125.40^\circ$ | $-1.02^\circ$ | $196.54^\circ$ |

## III. RESULTS & ANALYSIS

### 1. Disturbed Period

#### 1.1. Coronal holes (CH) events

##### 1.1.1. Case study 1: Observation period on 12 July 2009 to 18 July 2009

During period of case study 1, the event of coronal hole occurred on 13 July 2009 [11]. Based on Figure 2, it can be seen that starting from 13 July 2009 there is a sudden increase in the readings of the solar wind parameters. The sudden increment started with proton density,  $N$  at 0900 UT and followed by the IMF magnitude,  $B$  with delay of 1 hour while IMF temperature,  $T$  started at 1400 UT. Proton density is maximum on 13 July 2009 (1400 UT) with value of

$19.9 \text{ N/cm}^3$ . This is followed by the magnitude of IMF which reached its maximum of  $10.2 \text{ nT}$  on 13 July 2009 (1900 UT). At 2300 UT on the same day, the temperature of IMF increased to  $3.339 \times 10^5 \text{ K}$ . The solar wind speed reached its maximum by a delay of 5 hours on 14 July 2009 at 0400 UT with reading of  $540 \text{ km/s}$ . The readings of solar wind speed for this period varies and fluctuated from  $288 \text{ km/s}$  to  $540 \text{ km/s}$ . The solar wind input energy varies randomly all the day. The solar wind input energy started to increase on 13 July 2009 at 1200 UT. The maximum value of  $\varepsilon$  is up to  $3.028 \times 10^{18} \text{ ergs/s}$  occurred on 14 July 2009 at 0200 UT. 2 hours later at 0400 UT the solar wind input energy reading dropped to  $1.269 \times 10^{15} \text{ ergs/s}$ .

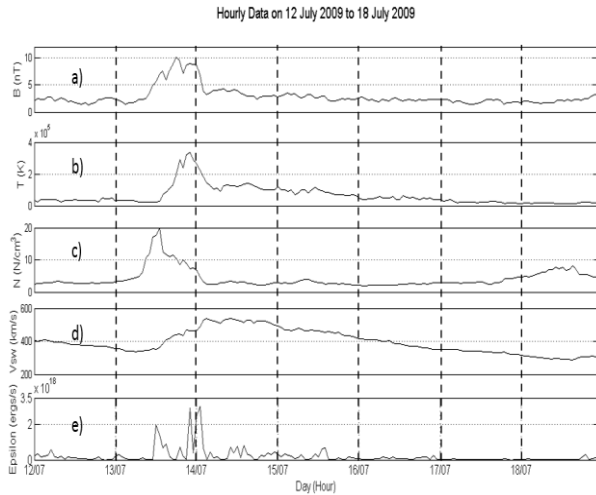


Figure 2: a) IMF Magnitude, B (nT), b) IMF Temperature, T (K), c) Proton Density, N, d) Solar Wind Speed, Vsw (km/s), d) Solar Wind Input Energy,  $\epsilon$  (ergs/s).

According to Figure 3, the polar cap index (PC), auroral electrojet index (AE), and planetary K-index (Kp) reaches their maximum at 14 July 2009 on 0200 UT. The PC index, AE index and Kp index reached maximum on the same time with maximum of  $\epsilon$  whereas there is delay of 1 hour for the Dst index. The maximum value of PC index is 2.3, AE index is 671 nT while Kp index is 37 nT. On the other hand, the Dst reached its minimum negative value with delay of 1 hour at 0300 UT on the same day. The Dst index of this period varies below than 21nT and reaching down to -25nT. The highest positive variation of Dst index is 21nT which occurred on 13 July 2009. By referring to Figure 2(e), the solar wind input energy experienced sudden increment at 1200 UT on 13 July 2009. Based on this variation, it can be seen that the PC index, AE index, and Kp index experienced sudden increment at the same time with  $\epsilon$  without any delay. However, Dst index experience the sudden increment by a delay of an hour at 1300 UT.

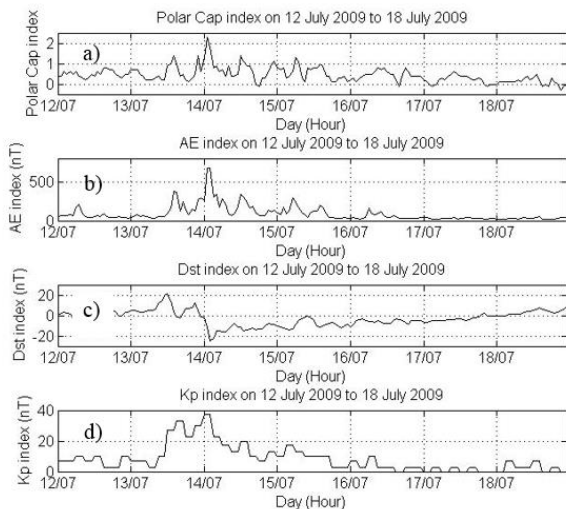


Figure 3: Geomagnetic indices. a) Polar Cap index (PC), b) Auroral electrojet index (AE) c) Disturbance Storm Time index (Dst) d) Planetary K-index (Kp).

Figure 4 shows the variations of geomagnetic pulsations, Pc5 of H-direction at different latitudes of MAGDAS

stations. Stations at high latitude, Magadan (MGD) (Figure 4(a)) and low latitude, Davao (DAV) (Figure 4(c)) experienced higher variations compared to mid latitude station. MAGDAS station at mid latitude, Onagawa (ONW) (Figure 4(b)) shows the least variations. Higher variations of Pc5 on 13 to 14 July occurred at all three stations shows that there is an event occurred during that day. The highest value reached by MGD station during coronal holes event is 3.219nT whereas DAV station reached maximum with value of 5.43nT. Mid latitude station, ONW reached maximum value of 1.434nT on 13 July 2009. The approximate percentage increase of Pc5 at MGD is 308%, 378% at ONW and 503% at DAV.

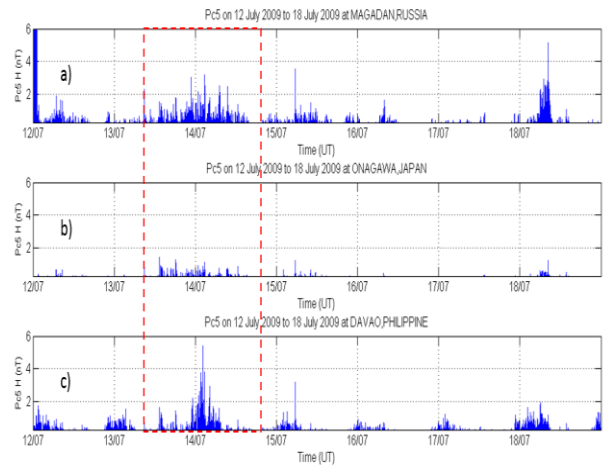


Figure 4: Pc5 of H-direction geomagnetic field at different latitudes MAGDAS stations a) High latitude station, b) Mid latitude station, c) Low latitude station.

### 1.1.2. Case study 2: Observation period on 14 June 2010 to 20 June 2010

During period of case study 2, the event of coronal holes occurred on 15 June 2010 [11]. Based on Figure 5, it can be seen that on 15 June 2010 there is a sudden increase in the readings of the solar wind parameters. The sudden increment started with proton density, N at 0400 UT and followed by the IMF magnitude, B with delay of 5 hours while IMF temperature, T started at 1100 UT. Proton density, N is maximum on 15 June 2010 (0900 UT) with value of 29.3 N/cm<sup>3</sup>. This is followed by the magnitude of IMF, B which reached its maximum of 10.7nT on 15 June 2010 (1500 UT). At 0900 UT on the same day, the temperature of IMF, T started to increase and reached maximum of 2.473x10<sup>5</sup> K on 16 June 2010 at 0400 UT. The solar wind speed, Vsw reached its maximum on 16 June 2010 at 2300 UT with reading of 571 km/s. The readings of solar wind speed for this period varies and fluctuated from 358 km/s to 571 km/s. The solar wind input energy,  $\epsilon$  varies randomly all the day. It experienced sudden increase at 2100 UT on 15 June 2010. The maximum value of  $\epsilon$  is up to 4.367x10<sup>18</sup> ergs/s occurred on 16 June 2010 at 0500 UT. 3 hours later, at 0800 UT the solar wind input energy,  $\epsilon$  reading dropped to 7.801x10<sup>17</sup> ergs/s.

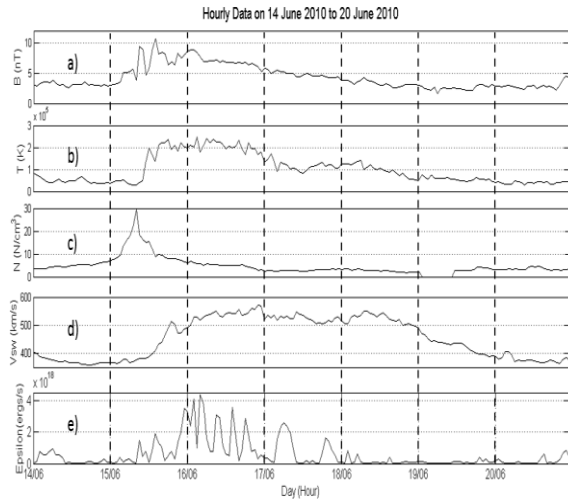


Figure 5: a) IMF Magnitude, B (nT), b) IMF Temperature, T (K), c) Proton Density, N, d) Solar Wind Speed, Vsw (km/s), d) Solar Wind Input Energy,  $\epsilon$  (ergs/s).

According to Figure 6, the polar cap index (PC) index and auroral electrojet index (AE) reaches their maximum at 16 June 2010 on 0300 UT. The PC index and AE index reached maximum on the same time with maximum of  $\epsilon$  (Figure 5 (e)) whereas there is delay of 1 hour for the Dst index. The maximum value of PC index is 2.3 whereas AE index is 727 nT. On the other hand, the Dst index reached its minimum negative value with delay of 1 hour at 0400 UT on the same day. The Dst index of this period varies below than 25nT and reaching down to -30nT. The highest positive variation of Dst index is 25nT which occurred on 16 June 2010. The highest reading of Kp index is 37 nT on 16 June at 2000 UT. By referring to Figure 5(e), the solar wind input energy,  $\epsilon$  experienced sudden increment at 2100 UT on 15 June 2010. Based on this variation, it can be seen that the PC index, AE index, and Kp index experienced sudden increment at the same time with  $\epsilon$  without any delay. However, Dst index start entering the main phase (start to decrease) at 2000 UT.

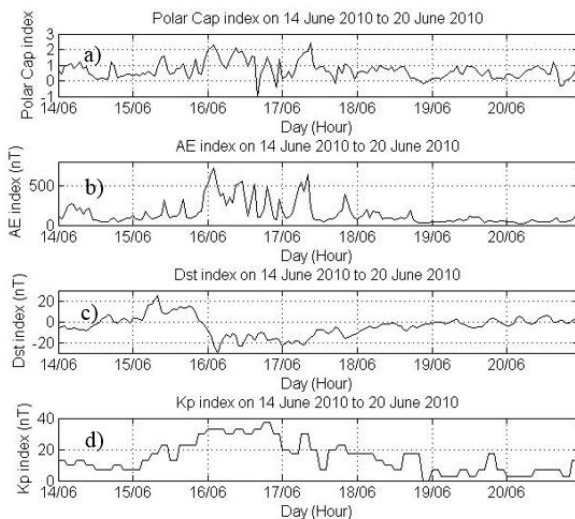


Figure 6: Geomagnetic indices. a) Polar Cap index (PC), b) Auroral Electrojet index (AE) c) Disturbance Storm Time index (Dst) d) Planetary K-index (Kp).

Figure 7 shows the variations of geomagnetic pulsations,

Pc5 of H-direction at different latitudes of MAGDAS stations. Stations at high latitude, Magadan (MGD) (Figure 7(a)) and low latitude, Davao (DAV) (Figure 7(c)) experienced higher variations compared to mid latitude station. MAGDAS station at mid latitude, Onagawa (ONW) (Figure 7(b)) shows the least variations. Higher variations of Pc5 on 15 to 16 June occurred at all three stations shows that there is an event occurred during that day. The highest value reached by MGD station during coronal holes event is 5.97nT whereas DAV station reached maximum with value of 4.888nT. Mid latitude station, ONW reached maximum value of 1.677nT on 15 June 2010. The approximate percentage increase of Pc5 at MGD is 298%, 319% at ONW and 253% at DAV.

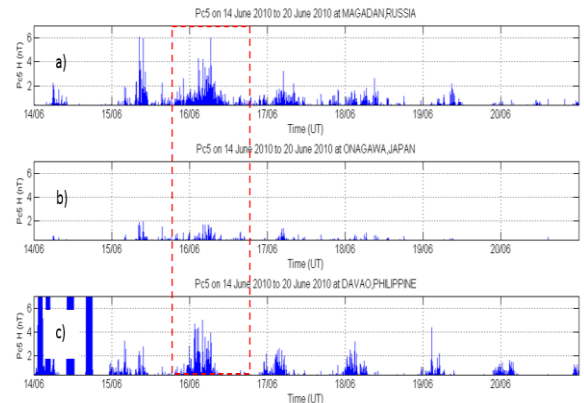


Figure 7: Pc5 of H-direction geomagnetic field at different latitudes MAGDAS stations a) High latitude station, b) Mid latitude station, c) Low latitude station.

## 1.2. Coronal Mass Ejection (CME)

### 1.2.1. Case study 1: Observation period on 01 August 2010 to 07 August 2010

During period of case study 1, the event of coronal mass ejection occurred on 3 August 2010 [12]. Based on Figure 8, it can be seen that on 3 August 2010 there is a sudden increase in the readings of the solar wind parameters. The sudden increment started with proton density, N at 1700 UT and followed by the IMF magnitude, B on the same time while IMF temperature, T started at 1800 UT. The IMF temperature, T is maximum on 3 August 2010 (2100 UT) with value of  $4.005 \times 10^5$  K. This is followed by the solar wind speed, Vsw that reached its maximum by a delay of 1 hour at 2200 UT with reading of 598 km/s. The readings of solar wind speed, Vsw for this period varies and fluctuated from 388 km/s to 598 km/s. The magnitude of IMF, B reached its maximum of 17.3nT on 4 August 2010 (0800 UT). At 0900 UT, the proton density, N reached maximum of 17.1 N/cm<sup>3</sup> on 4 August 2010. The solar wind input energy,  $\epsilon$  varies randomly all the day. It started its sudden increase at 1900 UT on 3 August 2010. The maximum value of  $\epsilon$  is up to  $1.397 \times 10^{19}$  ergs/s occurred on 3 August 2010 at 2200 UT. 2 hours later, at 0000 UT on 4 August 2010 the solar wind input energy reading dropped to  $3.257 \times 10^{18}$  ergs/s.

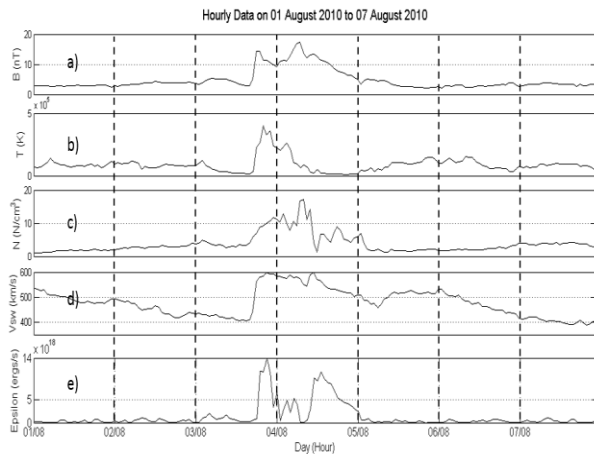


Figure 8: a) IMF Magnitude, B (nT), b) IMF Temperature, T (K), c) Proton Density, N, d) Solar Wind Speed, Vsw (km/s), d) Solar Wind Input Energy,  $\epsilon$  (ergs/s).

According to Figure 9, the polar cap index (PC) and planetary K-index (Kp) reaches their maximum on 3 August 2010 at 2200 UT. The PC index and Kp index reached maximum on the same time with maximum of  $\epsilon$  (Figure 8(e)) whereas there is delay of 2 hours for the Dst index. The highest reading of Kp index is 71 nT while PC index is 4.60. The Dst index of this period varies below than 20nT and reaching down to -67nT. The highest positive variation of Dst index is 20nT which occurred on 3 August 2010 at 2000 UT. Dst reached its minimum negative value with delay of 2 hours at 0000 UT on 4 August 2010. From the Dst index, the value of geomagnetic storm can be classified as moderate (-50nT to -100nT). The AE index reached its maximum on 4 August 2010 at 1500 UT. The maximum value reached by AE index is 1106 nT. By referring to Figure 8(e), the solar wind input energy experienced sudden increment at 1900 UT on 3 August 2010. Based on this variation, it can be seen that the PC index and AE index experienced sudden increment on the same time with  $\epsilon$  without any delay. However, Dst index start entering the main phase (start to decrease) by a delay of an hour at 2000 UT.

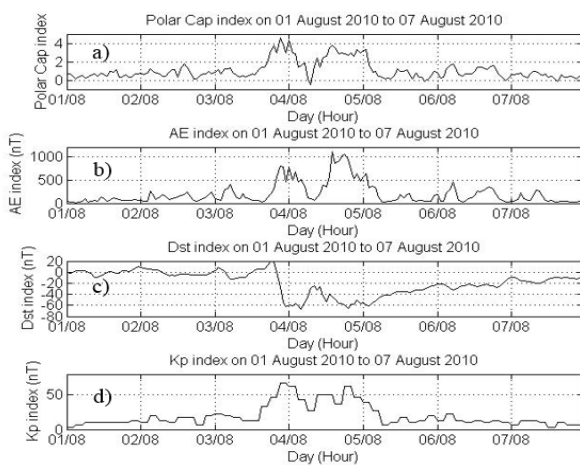


Figure 9: Geomagnetic indices. a) Polar Cap index (PC), b) Auroral Electrojet index (AE) c) Disturbance Storm Time index (Dst) d) Planetary K-index (Kp).

Figure 10 shows the variations of geomagnetic pulsations, Pc5 of H-direction at different latitudes of

MAGDAS stations. Stations at high latitude, Magadan (MGD) (Figure 10(a)) and low latitude, Davao (DAV) (Figure 10(c)) experienced higher variations compared to mid latitude stations. MAGDAS station at mid latitude, Onagawa (ONW) (Figure 10(b)) shows the least variations. Higher variations of Pc5 on 15 to 16 June occurred at all three stations shows that there is an event occurred during that day. Station at high latitude, MGD and low latitude station, DAV reached its maximum on 4 August 2010. The highest value reached by MGD station during coronal mass ejection event is 37.72nT whereas DAV station reached maximum with value of 26.45nT. Mid latitude station, ONW reached maximum value of 9.396nT on 3 August 2010. The approximate percentage increase of Pc5 at MGD is 300%, 800% at ONW and 211% at DAV.

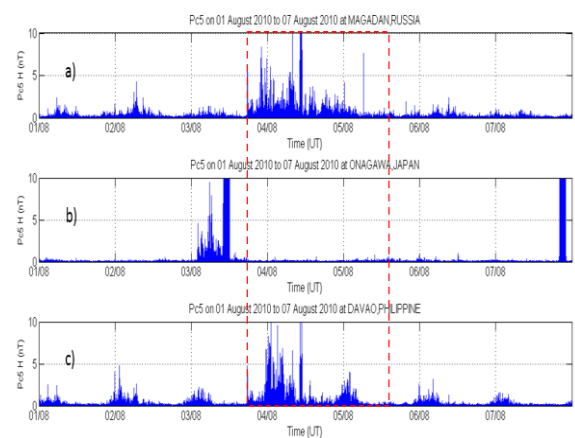


Figure 10: Pc5 of H-direction geomagnetic field at different latitudes of MAGDAS stations a) High latitude station, b) Mid latitude station, c) Low latitude station.

### 1.2.2. Case study 2: Observation period on 20 July 2009 to 26 July 2009

During period of case study 2, the event of coronal mass ejection occurred on 22 July 2009 [13]. Based on Figure 11, it can be seen that on 22 July 2009 there is a sudden increase in the readings of the solar wind parameters. The sudden increment started with proton density, N at 2000 UT and followed by the IMF magnitude, B with delay of 1 hour as well as the IMF temperature, T which started at 2200 UT. The proton density, N is maximum on 22 July 2009 (0600 UT) with value of 38.3 N/cm<sup>3</sup>. This is followed by the magnitude of IMF, B which reached its maximum of 16.7nT on 22 July 2009 (0700 UT). The temperature of IMF, T increased to 2.578x10<sup>5</sup> K on 23 July 2009 at 1300 UT. The solar wind speed, Vsw reached its maximum on 24 July 2009 at 0600 UT with reading of 575 km/s. The readings of solar wind speed for this period varies and fluctuated from 284 km/s to 575 km/s. The solar wind input energy varies randomly all the day. It experienced sudden increase at 0100 UT on 22 July 2009. The maximum value of  $\epsilon$  is up to 1.724x10<sup>19</sup> ergs/s occurred on 22 July 2009 at 0500 UT. 2 hours later, at 0700 UT on 22 July 2009 the solar wind input energy reading dropped to 1.96x10<sup>18</sup> ergs/s.

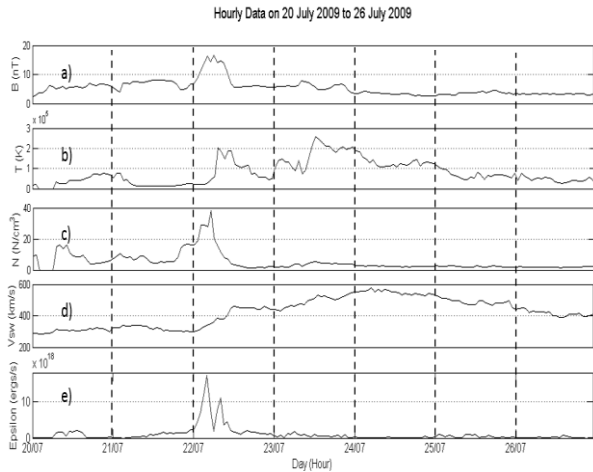


Figure 11: a) IMF Magnitude, B (nT), b) IMF Temperature, T (K), c) Proton Density, N, d) Solar Wind Speed, Vsw (km/s), d) Solar Wind Input Energy,  $\epsilon$  (ergs/s).

According to Figure 12, the polar cap index (PC), auroral electrojet index (AE), and planetary K-index (Kp) reaches their maximum at 22 July 2009 at 0500 UT. The PC index, AE index and Kp index reached maximum on the same time with maximum of  $\epsilon$  whereas there is delay of 2 hours for the Dst index. The maximum value of PC index is 4.1 while AE index is 1058 nT. The highest reading of Kp index is 57 nT. The Dst index of this period varies below than 14nT and reaching down to -83nT. On the other hand, the Dst reached its minimum negative value with delay of 2 hours at 0700 UT on the same day. The highest positive variation of Dst index is 14nT which occurred on 20 July 2009. By referring to Figure 11(e), the solar wind input energy experienced sudden increment at 0100 UT on 22 July 2009. Based on this variation, it can be seen that the PC index, AE index, and Kp index experienced sudden increment at the same time with  $\epsilon$  without any delay. However, Dst index start entering the main phase (start to decrease) by a delay of an hour at 0200 UT. Based on the variation of Dst, it can be classified as moderate geomagnetic storm since the Dst index is in the range of  $-50 \text{ nT} < \text{peak Dst} < -100 \text{ nT}$ .

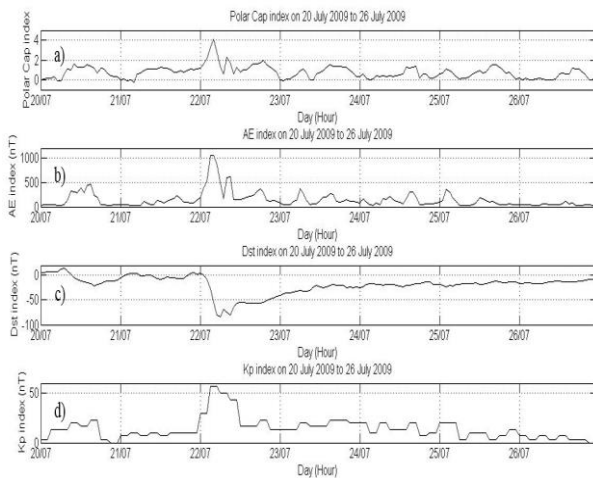


Figure 12: Geomagnetic indices. a) Polar Cap index (PC), b) Auroral Electrojet index (AE) c) Disturbance Storm Time index (Dst) d) Planetary K-index (Kp).

Figure 13 shows the variations of geomagnetic pulsations, Pc5 of H-direction at different latitudes of MAGDAS stations. Stations at high latitude, Magadan

(MGD) (Figure 13(a)) and low latitude, Davao (DAV) (Figure 13(c)) experienced higher variations compared to mid latitude station. MAGDAS station at mid latitude, Onagawa (ONW) (Figure 13(b)) shows the least variations. Higher variations of Pc5 on 22 July 2009 occurred at all three stations shows that there is an event during that day. Station at high latitude, MGD and mid latitude station, ONW reached its maximum on 22 July 2010. The highest value reached by MGD station during coronal mass ejection event is 6.265nT whereas DAV station reached maximum with value of 5.725nT. Mid latitude station, ONW reached maximum value of 1.479nT on 20 July 2010. The approximate percentage increase of Pc5 at MGD is 422%, 195% at ONW and 340% at DAV.

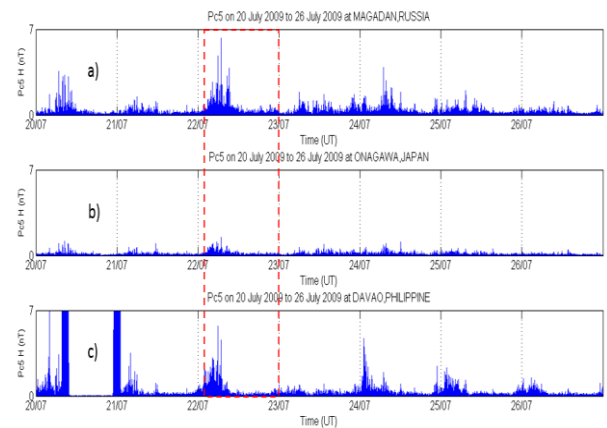


Figure 13: Pc5 of H-direction geomagnetic field at different latitudes MAGDAS stations a) High latitude station, b) Mid latitude station, c) Low latitude station.

## 2. Quiet Period

### 2.1. Case study 1: Observation period on 10 August 2009 to 16 August 2009

During case study of quiet period, there is no sudden increment in the solar wind parameters and geomagnetic activity. By referring to Figure 14 (a), the highest reading of solar wind dynamic pressure is recorded on the 11 of August 2009 in which the dynamic pressure is 1.73nPa. The solar wind dynamic pressure varies and fluctuated between 0.7 nPa and 1.73 nPa within this study case period.

The solar wind speed distribution varies from 267km/s to 389km/s as shown in Figure 14 (b). The speed of solar wind is at maximum during 10 August 2009 by which the reading reached 389km/s. It is classified as quiet period for the day with solar wind speed lower than 400km/s. Solar wind speed on earth is normally occur around 300km/s but can be highly increase if coronal mass injection or coronal holes arrives. Based on this graph, there is no coronal mass injection or coronal holes events occurred because the highest speed is only 389km/s and there is no sudden increment of the speed. Therefore, it can be classified as quiet period for this observation period.

The solar wind input energy varies randomly all the day.

Figure 14 (c) shows the variations of solar wind input energy,  $\epsilon$  on 10 August 2009 to 16 August 2009. The solar wind input energy varies randomly along this period. The maximum range value of  $\epsilon$  is up to  $6.943 \times 10^{17}$  ergs/s on 12 August 2009 (1200 UT). The solar wind input energy reaches peaks on 11 August (1800 UT), 12 August (1200 UT & 2100 UT), 13 August (1300 UT) and 14 August (0900 UT).

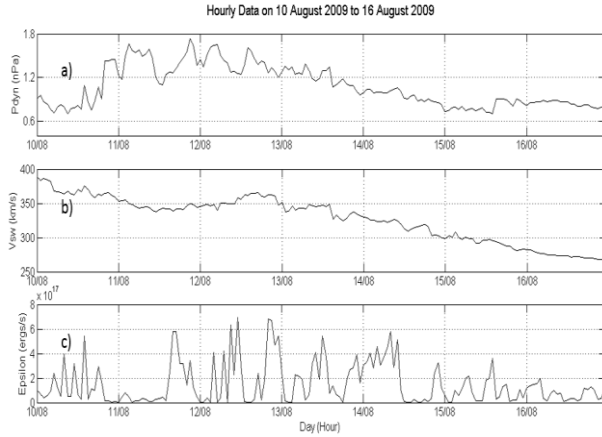


Figure 14: a) Solar Wind Dynamic Pressure (nPa), b) Solar Wind Speed,  $V_{sw}$  (km/s), c) Solar Wind Input Energy,  $\epsilon$  (ergs/s).

Based on Figure 15, the variations of PC index, AE index and Kp index have higher readings on 11 August (1800 UT), 12 August (1200 UT & 2100 UT), 13 August (1300 UT) and 14 August (0900 UT). Dst index value also reaches minimum negative values on the same time but with a delay of 1 hour. The Dst index of this period varies below than 4nT and reaching down to -15nT as referred to Figure 15 (c). Based on the variation of Dst, it can be categorized as quiet since the Dst index is around the range of  $-20 < \text{peak Dst} < +20$ . These geomagnetic indices varies simultaneously similar to the variations of the solar wind input energy,  $\epsilon$  (Figure 14 (c)) and the solar wind dynamic pressure,  $P_{dyn}$  (Figure 14 (a)). This clarify that the variations of the geomagnetic indices are associated with the solar wind parameters.

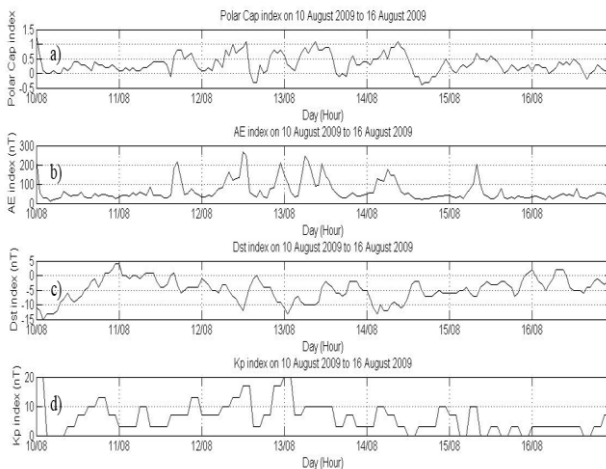


Figure 15: Geomagnetic indices. a) Polar Cap index (PC), b) Auroral Electrojet index (AE) c) Disturbance Storm Time index (Dst) d) Planetary K-index (Kp).

Figure 16 shows the variations of geomagnetic pulsations, Pc5 of H-direction at different latitudes of MAGDAS stations. Stations at high latitude, Magadan (MGD) and

low latitude, Davao (DAV) experienced higher variations compared to mid latitude stations. MAGDAS station at mid latitude, Onagawa (ONW) shows the least variations. There is no event occurred during this period as there is no sudden increase in the variations.

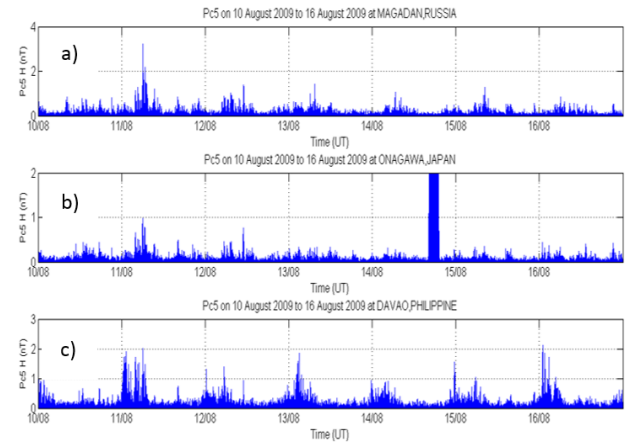


Figure 16: Pc5 of H-direction geomagnetic field at different latitude MAGDAS stations a) High latitude station, b) Mid latitude station, c) Low latitude station.

#### IV. DISCUSSIONS

The present work has been made to achieve a better understanding of the solar wind parameters and their relationships with various geomagnetic indices during disturbed and quiet period. Two events of coronal holes and coronal mass ejections was investigated in a time interval of 7 days for each event to examine the variations of solar wind parameters, geomagnetic indices and geomagnetic pulsations.

Characteristics of coronal holes (CH) and coronal mass ejection (CME) were determined based on several solar wind parameters. The solar wind parameters that is significant to characterize CH and CME are the IMF magnitude,  $B$ , IMF temperature,  $T$ , proton density,  $N$ , and solar wind speed,  $V_{sw}$ . Events of CH and CME during disturbed period lead to the sudden increment of these solar wind parameters. At the beginning, the proton density,  $N$  will experienced sudden increment which later followed by the IMF magnitude,  $B$  and IMF temperature,  $T$  with a short delay.

The variation of the solar wind speed,  $V_{sw}$  can be used to characterize events of coronal holes or coronal mass ejection. The solar wind speed will reach peaks slowly and remains for a longer period for coronal holes event (Figure 2 (d) & 5(d)) whereas for coronal mass ejection, the enhancement of  $V_{sw}$  is faster to reach peak and remains for shorter period of time (Figure 8 (d) & 11 (d)) [3].

Based on the analysis, PC index, AE index, and Kp index experienced sudden increment at the same time with solar wind input energy,  $\epsilon$  without any delay. However, Dst index start entering the main phase (start to decrease) by delay of 1 to 2 hours. This delay is due to the different latitudes location of the index measurements. The PC index measures geomagnetic disturbances at the polar cap, AE index are measured from northern hemisphere auroral zone, Dst index is obtained from magnetometer stations near the equator



while Kp index is obtained from a number of magnetometer stations at mid-latitudes.

Both coronal holes and coronal mass ejection influenced the variations of the earth's horizontal magnetic field at all latitudes. Higher latitude station experience higher variations compared to mid latitude station is due to the penetration of solar wind input energy from the North Pole. High latitude station and low latitude station experienced higher variation of geomagnetic pulsation, Pc5 compared to mid latitude station. This results are due to several reasons such as the Kelvin-Helmholtz instability, broad-band pulses, and fluctuations of the solar wind dynamic pressure [14].

## V. CONCLUSIONS

On the basis of observational results and discussions, important conclusions have been summarized. Higher variations of solar wind parameters and geomagnetic indices are due to the activities of coronal holes and coronal mass ejections. Both coronal holes and coronal mass ejection events lead to the high solar wind input energy that penetrate towards the earth. However, coronal mass ejection caused higher solar wind input energy to penetrate to the earth as compared to coronal holes. The variations of geomagnetic indices are associated with the solar wind parameters (solar wind input energy and solar wind dynamic pressure). The occurring of the geomagnetic pulsations can be determine based on the solar wind parameters. The results shows that Pc5 is a suitable index to study the relationship of solar wind parameters with the earth geomagnetic.

## ACKNOWLEDGMENT

The author are grateful to the MAGDAS/CPMN Group by International Center for Space Weather Science and Education (ICSWSE), Kyushu University, Japan for providing the geomagnetic data and National Space Agency for maintaining the equipment. The author also want to thank OMNIWeb Data Explorer, Space Physics Data Facility from NASA for providing the data of solar wind parameters and geomagnetic indices. Indebted gratitude and deepest thanks to Dr. Huzaimy Jusoh, research supervisor for all the supports and guidance. Special thanks to the Space & Earth's Electromagnetism (SEE) Group Uitm Shah Alam.

## REFERENCES

- [1] Burkepile, J., "An introduction to space weather", High Altitude Observatory/ NCAR.
- [2] Steven R Cranmer, "Coronal Holes ", Encyclopedia of Astronomy and Astrophysics Nature, pp. 1-6, 2000.
- [3] V. Gupta and Badruddin, "High-Speed Solar Wind Streams during 1996-2007: Sources, Statistical Distribution, and Plasma/Field Properties", Springer Netherlands, pp. 165-188, 2010.
- [4] Byrne, Jason P. "The Kinematics and Morphology of Solar Coronal Mass Ejections." *arXiv preprint arXiv:1202.4005*, 2012.
- [5] Troshichev, O. A., O. Rasmussen, and V. O. Papitashvili. "Polar Cap (PC) Magnetic Activity Index." ACE Real Time Solar Wind Data, *Auroral Electrojet Index (AE)*. [cited 2014 29/05/2014]; Retrieve from: <http://www.ngdc.noaa.gov/stp/geomag/ae.html>.
- [6] Lin, J.-W., "Ionospheric Anomaly after the 11 April, 2012, M =8.6 Indonesia' Sumatra Earthquake Using Two-Dimensional Principal Component Analysis (2DPCA)", *Journal of Scientific Research & Reports*, Vol. 3, No. 1, pp. 204-226, 2014.
- [7] Gannon, J. L., et al. "US Geological Survey near real-time Dst index." *US Geol. Surv. Open File Rep* 1030 (2011): 13.
- [8] Perreault, Paul, and S. I. Akasofu. "A study of geomagnetic storms." *Geophysical Journal International* 54.3 (1978): 547-573.
- [9] Space Environment Research Center, "MAGDAS Map and Stations", Retrieve from: <http://magdas2.serc.kyushu-u.ac.jp/station/>.
- [10] Dr. Tony Phillips., "What's up in space", Retrieve from: <http://www.spaceweather.com/>.
- [11] NASA Official, "Spacecraft Observes Coronal Mass Ejection", Retrieve from: <http://www.nasa.gov/topics/solarsystem/sunearthssystem/main/news080210-cme.html#U4fYafmSynk>.
- [12] Bosman, E., et al. "Three-Dimensional Properties of Coronal Mass Ejections from STEREO/SECCHI Observations." *Solar Physics* 281.1 (2012): 167-185.
- [13] Francia, P., et al. "ULF geomagnetic pulsations at different latitudes in Antarctica." *Annales Geophysicae*. Vol. 27. No. 9. Copernicus GmbH, 2009.